Iranian Journal of Numerical Analysis and Optimization
Vol. ??, No. ??, ??, pp ??
https://doi.org/??
https://ijnao.um.ac.ir/

Research Article

Mathematical modeling and control strategies for meningitis transmission

M. Baroudi*, B. Bettioui, M. Belam and A. Labzai

Abstract

Meningitis is one of the world's most alarming infectious diseases, characterized by rapid progression, high fatality, and severe long-term complications. Despite advances in vaccination and surveillance, recurrent epidemics—especially across Africa's "meningitis belt"—continue to threaten millions. This study introduces a novel compartmental model, $SEAIVHRQ$, integrating both medical and behavioral aspects of meningitis dynamics. The model divides

*Corresponding author

Received ??? ; revised ??? ; accepted ???

Mohamed Baroudi
Laboratory of Advanced Research in Industrial and Logistic Engineering (LARILE), Applied Mathematics Team, Department of Mathematics and Computer Science, ENSEM, Hassan II University of Casablanca, Morocco. e-mail: m.mohamed.baroudi@gmail.com

Benyounes Bettioui
Centre Régional des Métiers de l'Éducation et de la Formation (CRMEF), 20340 Derb Ghalef, Casablanca, Maroc. e-mail: benyounes.bettioui@gmail.com

Mohamed Belam
Laboratory of Advanced Research in Industrial and Logistic Engineering (LARILE), Applied Mathematics Team, Department of Mathematics and Computer Science, ENSEM, Hassan II University of Casablanca, Morocco. e-mail: m.belam@gmail.com

Abderrahim Labzai
Laboratory of Analysis Modeling and Simulation, Department of Mathematics and Computer Science, Faculty of Sciences Ben M'sik, Hassan II University of Casablanca, Morocco. e-mail: labzaiabdo1977@gmail.com

How to cite this article
Baroudi, M., Bettioui, B., Belam, M. and Labzai, A., Mathematical modeling and control strategies for meningitis transmission. *Iran. J. Numer. Anal. Optim.*, ??; ??(??): ??-??. ??

the population into eight classes, incorporating vaccination and voluntary quarantine to reflect realistic public health conditions. Three time-dependent controls are applied to reduce transmission from asymptomatic and symptomatic individuals and to enhance awareness and treatment adherence. Using Pontryagin's Maximum Principle, we determine optimal strategies that minimize infection prevalence, hospitalization, and intervention costs. Numerical simulations show that combined preventive, treatment, and awareness measures substantially reduce infection peaks and accelerate recovery. This framework extends classical models and supports the WHO's "Defeating Meningitis by 2030" roadmap, offering practical insights for designing cost-effective and sustainable control strategies in resource-limited health systems.

AMS subject classifications (2020): 49J15, 93C10, 92B05, 93A30.

Keywords: Meningitis; Pontryagin's maximum principle; MATLAB; Bacterial meningitis.

1 Introduction

Meningitis is a severe infection of the meninges, the protective membranes surrounding the brain and the spinal cord. According to the World Health Organization (WHO), bacterial meningitis is among the most devastating infectious diseases, causing high morbidity and mortality worldwide [1, 44, 4]. The main bacterial agents include *Neisseria meningitidis*, *Streptococcus pneumoniae*, *Haemophilus influenzae*, *Group B Streptococcus*, *Listeria monocytogenes*, *Escherichia coli*, and *Mycobacterium tuberculosis* [3, 4, 5]. Transmission typically occurs from person to person through coughing, sneezing, or close contact with infected individuals or asymptomatic carriers [1, 6, 7]. The clinical symptoms are characterized by a sudden onset of fever, headache, stiff neck, nausea, vomiting, photophobia, and confusion [1, 2]. The case fatality rate varies from 3–10% in developed countries to as high as 20% in the African "meningitis belt," a region stretching from Senegal to Ethiopia [2, 7, 8]. Moreover, nearly 20% of survivors may develop long-term neurological sequelae such as deafness, epilepsy, cerebral palsy, speech disorders, limb loss, or intellectual disability [1, 2]. These alarming statistics highlight the serious threat of meningitis to human health and justify the need for advanced strategies of prevention and control [9, 4, 10].

The WHO launched the global roadmap *"Defeating Meningitis by 2030"*, which aims to eliminate bacterial meningitis epidemics, reduce vaccine-preventable cases by 50%, cut mortality by 70%, and improve quality of life for those affected [4]. While remarkable progress has been made through vaccination campaigns, surveillance, and case management, challenges remain [9, 10, 7]. Outbreaks continue to occur, particularly during the dry season (November–May) in sub-Saharan Africa, where climatic conditions, population movements, and poverty exacerbate

transmission dynamics [2, 7, 8]. In this context, mathematical modeling provides a rigorous framework to understand disease dynamics, to test hypothetical scenarios in the absence of sufficient real-world data, and to design optimal strategies for epidemic control [6, 11, 5, 7, 8, 12].

Several studies in the literature have applied mathematical and optimal control approaches to meningitis and other infectious diseases [6, 11, 13, 5, 20, 23, 14, 15, 12, 16]. Deterministic compartmental models have been formulated to analyze co-infections, such as tuberculosis-hepatitis B, malaria-meningitis, hepatitis B-HIV, and pneumonia-meningitis [17, 19, 11, 13, 21, 18]. Simulation results from these studies consistently demonstrated that implementing preventive measures, treatment, and vaccination together can significantly reduce the burden of infection [19, 11, 13, 21, 18, 20, 15, 12, 16]. For example, Tilahun [42] developed an optimal control model for pneumonia and meningitis co-infection, showing that combined preventive and treatment strategies achieved substantial reductions in both diseases. Similarly, other researchers have investigated hepatitis B and hepatitis C co-infection under fractional-order models, highlighting the complexity of overlapping epidemics [21, 20, 23, 14, 15]. These works collectively underline the importance of designing robust control strategies adapted to the biological, social, and economic contexts of infectious diseases [5, 20, 8, 12, 16, 22, 24, 25, 26, 27, 30, 28, 29].

In this study, we focus on a $SEAIVHRQ$ model tailored to meningitis transmission. This model subdivides the population into the following compartments: Susceptible (S), Exposed (E), Asymptomatic infected (A), Symptomatic infected (I), Vaccinated (V), Hospitalized (H), Recovered (R), and Quarantined (Q). The introduction of compartment Q is a key innovation in this work: It accounts for individuals who are infected but prefer to remain at home rather than seek hospital care, reflecting the reality of quarantine and self-isolation in resource-limited settings. Similarly, the compartment V represents individuals vaccinated at the onset, highlighting the role of proactive immunization. These additions make the model more realistic and allow for the assessment of both medical and behavioral interventions.

To improve epidemic control, we incorporate three time-dependent control functions:

- $c_1(t)$: reducing transmission from asymptomatic carriers (A), who often spread infection silently within communities.

- $c_2(t)$: reducing transmission from symptomatic individuals (I) through isolation, treatment, and limiting their contact with healthy individuals.

- $c_3(t)$: promoting awareness and responsibility, which includes ensuring access to medications at home, clear explanations of dosage, and stressing the importance of completing treatment.

These controls reflect practical strategies such as vaccination, isolation, quarantine, awareness campaigns, and logistic support for home-based care. By simulating different combinations of controls, we aim to identify the most effective strategies for minimizing infections, reducing mortality, and optimizing healthcare resource use.

The value of this study lies in extending classical meningitis models to include realistic features such as voluntary quarantine and proactive vaccination, and in analyzing their impacts under optimal control theory. By doing so, we provide insights into how to balance preventive measures, treatment interventions, and awareness programs in a cost-effective manner. This approach aligns with global health objectives, particularly the WHO's 2030 roadmap, and offers practical implications for policymakers in regions where meningitis remains a pressing public health challenge.

The remainder of this article is organized as follows. In Section 2, we present the formulation of the SEAIVHRQ model, defining state variables and parameters. Section 3 introduces the controlled mathematical model and discusses its qualitative properties. Section 4 addresses the challenge of identifying the optimal control strategies and outlines the algorithm employed. Section 5 provides numerical simulations to illustrate the effects of different control categories and compares their effectiveness. Finally, Section 6 offers concluding remarks and perspectives for future work.

2 Formulation of the model

In this work, we formulated the $SEAIVHRQ$ compartmental model to describe the transmission dynamics of meningitis within a human population.

For this purpose, the total population N is stratified into distinct epidemiological classes: Susceptible individuals S, exposed individuals E, asymptomatic infected individuals A, symptomatic infected individuals I, vaccinated individuals V, hospitalized individuals H, recovered individuals R, and quarantined individuals Q. The overall human population at time t is expressed as $N = S + E + A + I + V + H + R + Q$. A schematic diagram representing the flow between compartments in the proposed model is presented in Figure 1.

Compartment S: The $S(t)$ compartment represents the susceptible population who can contract the disease. The inflow comes from new recruits $\Sigma(1-\alpha)$, while the outflow occurs as susceptible individuals become exposed due to contact with symptomatic infected individuals $\beta_1 \frac{SI}{N}$ or asymptomatic infected individuals $\beta_2 \frac{SA}{N}$. In addition, natural mortality μ decreases this compartment, and some susceptibles move into the vaccinated class V at rate k_1.

Compartment V: The $V(t)$ compartment represents vaccinated individuals who are protected

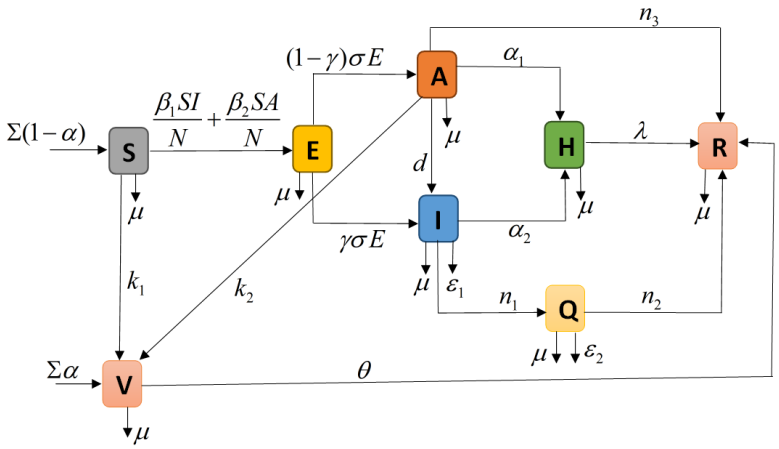

Figure 1: Model of population compartments.

from infection. This class increases through direct vaccination $\Sigma\alpha$, as well as vaccination of susceptible individuals at rate $k_1 S$ and asymptomatic individuals at rate $k_2 A$. The compartment decreases due to vaccine waning at rate θ and natural mortality μ.

Compartment E: The $E(t)$ compartment denotes the exposed individuals who have been infected but are not yet infectious. They are generated from susceptible individuals S through interactions with both symptomatic I and asymptomatic A infections. They progress to either the asymptomatic class A at rate $(1-\gamma)\sigma E$ or the symptomatic class I at rate $\gamma\sigma E$, and the compartment decreases due to natural mortality μ.

Compartment A: The $A(t)$ compartment represents asymptomatic infected individuals who can still transmit the infection. It increases as a fraction $(1-\gamma)\sigma E$ of exposed individuals become asymptomatic. The compartment decreases due to disease progression to the symptomatic class I at rate d, hospitalization at rate α_1, quarantine at rate n_3, and natural mortality μ.

Compartment I: The $I(t)$ compartment describes symptomatic infected individuals. It increases when a fraction $\gamma\sigma E$ of exposed individuals develop symptoms, and also when asymptomatic individuals A progress to symptomatic infection at rate d. The outflow occurs through hospitalization at rate α_2, disease-induced death ε_1, transfer to quarantine n_1, and natural mortality μ.

Compartment H: The $H(t)$ compartment represents hospitalized individuals. It receives inflow from asymptomatic individuals hospitalized at rate α_1 and symptomatic individuals hospitalized at rate α_2. The compartment decreases as patients either recover at rate λ or die from natural mortality μ.

Compartment R: The $R(t)$ compartment denotes recovered individuals who have acquired

immunity. Recovery comes from hospitalized individuals at rate λ, quarantined individuals at rate n_2, and asymptomatic individuals at rate n_3. The compartment decreases due to natural mortality μ.

Compartment Q: The $Q(t)$ compartment represents individuals in quarantine who are isolated at home. They enter from the symptomatic class I at rate n_1 and exit either by recovering at rate n_2, dying due to disease ε_2, or through natural mortality μ.

We perform an analysis of a system consisting of eight nonlinear differential equations:

$$\begin{cases} \frac{dS}{dt} = \Sigma(1-\alpha) - \beta_1 \frac{SA}{N} - \beta_2 \frac{SI}{N} - (k_1+\mu)S, \\ \frac{dV}{dt} = \Sigma\alpha + k_1 S + k_2 A - (\theta+\mu)V, \\ \frac{dE}{dt} = \beta_1 \frac{SA}{N} + \beta_2 \frac{SI}{N} - (\sigma+\mu)E, \\ \frac{dI}{dt} = \gamma\sigma E + dA - (\alpha_2 + n_1 + \varepsilon_1 + \mu)I, \\ \frac{dA}{dt} = (1-\gamma)\sigma E - (d + n_3 + \alpha_1 + \mu + k_2)A, \\ \frac{dH}{dt} = \alpha_1 A + \alpha_2 I - (\lambda+\mu)H, \\ \frac{dR}{dt} = \lambda H + n_3 A + n_2 Q + \theta V - \mu R, \\ \frac{dQ}{dt} = n_1 I - (n_2 + \varepsilon_2 + \mu)Q, \end{cases} \tag{1}$$

where $(S(0), V(0), E(0), I(0), A(0), H(0), R(0), Q(0)) \in \mathbb{R}^8_+$ represents the specified initial state.

2.1 Fundamental model characteristics

2.1.1 Nonnegativity of solutions

Theorem 1. If the initial conditions satisfy $S(0) \geq 0$, $V(0) \geq 0$, $E(0) \geq 0$, $I(0) \geq 0$, $A(0) \geq 0$, $H(0) \geq 0$, $R(0) \geq 0$ and $Q(0) \geq 0$, then the solutions to system (1) remain positive for all $t \geq 0$.

Proof. By examining the first equation in system (1), it becomes clear that

$$\begin{aligned} \frac{dS(t)}{dt} &= \Sigma(1-\alpha) + \left(-\frac{\beta_1 A}{N} - \frac{\beta_2 I}{N} - (k_1+\mu)\right) S(t) \\ &\geq -\left(\frac{\beta_1 A}{N} + \frac{\beta_2 I}{N} + k_1 + \mu\right) S(t), \end{aligned}$$

$$\frac{dS(t)}{dt} + \left(\frac{\beta_1 A}{N} + \frac{\beta_2 I}{N} + k_1 + \mu\right) S(t) \geq 0,$$

where $N(t) = \frac{\beta_1 A}{N} + \frac{\beta_2 I}{N} + k_1 + \mu$.
We obtain

$$\frac{dS(t)}{dt} + N(t)S(t) \ \geq \ 0,$$

$$\exp\left(\int_0^t N(s)ds\right)\frac{dS(t)}{dt} + N(t)\exp\left(\int_0^t N(s)ds\right)S(t) \ \geq \ 0,$$

$$\frac{d}{dt}\left(S(t)\exp\left(\int_0^t N(s)ds\right)\right) \ \geq \ 0,$$

$$\int_0^t \left(\frac{d}{ds}\left(S(s)\exp\left(\int_0^t N(s)ds\right)\right)\right)ds \geq \ 0,$$

$$S(t) \geq S(0)\exp\left(-\int_0^t N(s)ds\right),$$

$$S(t) \geq 0.$$

In the same manner, we have

$$\frac{dV}{dt} + (\theta + \mu).V = \Sigma\alpha + k_1 S + k_2 V,$$

$$\begin{aligned}\exp\left((\theta+\mu)t\right).\frac{dV}{dt} + (\theta+\mu).\exp\left((\theta+\mu)t\right).V \\ = \left(\Sigma\alpha + k_1 S + k_2 V\right).\exp\left((\theta+\mu)t\right),\end{aligned}$$

which can be rewritten as

$$\frac{d}{dt}\left(V(t).\exp\left((\theta+\mu)t\right)\right) = \left(\Sigma\alpha + k_1 S + k_2 V\right).\exp\left((\theta+\mu)t\right),$$

thus,

$$V(t).\exp\left((\theta+\mu)t\right)-V(0)=\int_0^{t_1}\left(\Sigma\alpha+k_1S(x)+k_2V(x)\right).\exp\left((\theta+\mu)t\right)dx.$$

Therefore,

$$\begin{aligned}V(t)=&V(0).\exp\left(-(\theta+\mu)t\right)\\&+\exp\left(-(\theta+\mu)t\right).\int_0^{t_1}\left(\Sigma\alpha+k_1S+k_2V\right).\exp\left((\theta+\mu)t\right)dx\\\geq&0\end{aligned}$$

Similarly, we illustrate $E(t)\geq 0,\ I(t)\geq 0,\ A(t)\geq 0,\ H(t)\geq 0,\ R(t)\geq 0$ *and* $Q(t)\geq 0$. □

2.2 Boundedness of the solutions

Theorem 2. The collection

$$\Omega_h=\left\{(S,V,E,I,A,H,R,Q)\in\mathbb{R}_+^8:0\leq S+V+E+I+A+H+R+Q\leq\frac{\Sigma}{\mu}\right\}$$

ensures positive invariance within system (1) based on the given initial conditions $S(t)\geq 0,\ V(t)\geq 0,\ E(t)\geq 0,\ I(t)\geq 0,\ A(t)\geq 0,\ H(t)\geq 0,\ R(t)\geq 0$ *and* $Q(t)\geq 0$.

Proof. As specified, $N=S+V+E+I+A+H+R+Q$.

Therefore

$$\frac{dN}{dt}=\Sigma-\varepsilon_1I-\varepsilon_2Q-\mu N,$$

$$\frac{dN}{dt}=\Sigma-\varepsilon_1I-\varepsilon_2Q-\mu N\leq\Sigma-\mu N,$$

$$\frac{dN}{dt}\leq\Sigma-\mu N,$$

$$N(t)\leq(1-e^{-\mu t})\frac{\Sigma}{\mu}+N(0)e^{-\mu t}.$$

As $t \to \infty$, it follows that limit $t \to \infty \sup N(t) = \frac{\Sigma}{\mu}$. Consequently, the region Ω is confirmed to be a positively invariant set for system (1),

$$N(t) \leq \frac{\Sigma}{\mu}.$$

□

2.3 Existence and uniqueness of solutions

Theorem 3. System (1), with the initial conditions

$$(S(0), V(0), E(0), I(0), A(0), H(0), R(0), Q(0))$$

has a unique solution. This ensures that, for any given set of initial values within the defined range, the system's behavior can be accurately predicted.

Proof. System (1) can be expressed as follows: $\Theta(Y) = KY + L(Y)$, where

$$Y = \begin{pmatrix} S \\ V \\ E \\ I \\ A \\ H \\ R \\ Q \end{pmatrix}, \qquad L(Y) = \begin{pmatrix} \frac{dS}{dt} \\ \frac{dV}{dt} \\ \frac{dE}{dt} \\ \frac{dI}{dt} \\ \frac{dA}{dt} \\ \frac{dH}{dt} \\ \frac{dR}{dt} \\ \frac{dQ}{dt} \end{pmatrix}$$

and

$$K = \begin{pmatrix} -(k_1+\mu) & 0 & 0 & 0 & 0 & 0 & 0 & 0 \\ k_1 & -(\theta+\mu) & 0 & 0 & k_2 & 0 & 0 & 0 \\ 0 & & -(\sigma+\mu) & 0 & 0 & 0 & 0 & 0 \\ 0 & & \gamma\sigma & \omega_1 & d & 0 & 0 & 0 \\ 0 & 0 & (1-\gamma)\sigma & 0 & \omega_2 & 0 & 0 & 0 \\ 0 & 0 & 0 & \alpha_2 & \alpha_1 & -(\lambda+\mu) & 0 & 0 \\ 0 & \theta & 0 & 0 & n_3 & \lambda & -\mu & n_2 \\ 0 & 0 & 0 & n_1 & 0 & 0 & 0 & \omega_3 \end{pmatrix},$$

where $\omega_1 = -(\alpha_2 + n_1 + \varepsilon_1 + \mu)$, $\omega_2 = -(d + n_3 + \alpha_1 + \mu + k_2)$ *and* $\omega_3 = -(n_2 + \varepsilon_2 + \mu)$.

In addition to

$$L(Y) = \begin{pmatrix} \Sigma(1-\alpha) - \beta_1 \frac{SA}{N} - \beta_2 \frac{SI}{N} \\ \Sigma\alpha \\ \beta_1 \frac{SA}{N} + \beta_2 \frac{SI}{N} \\ 0 \\ 0 \\ 0 \\ 0 \\ 0 \end{pmatrix}.$$

□

Assuming that Y_1 and Y_2 are solutions of (1), it follows that

$$\begin{aligned} |L(Y_1) - L(Y_2)| &\leq 2\left|\beta_1 \frac{S_1 A_1}{N} + \beta_2 \frac{S_1 I_1}{N} - \beta_2 \frac{S_2 A_2}{N} - \beta_2 \frac{S_2 I_2}{N}\right| \\ &\leq 2\left|\frac{\beta_1 S_1}{N}(A_1 - A_2) + \frac{\beta_1 A_2}{N}(S_1 - S_2) + \frac{\beta_2 S_1}{N}(I_1 - I_2)\right. \\ &\quad \left. + \frac{\beta_2 I_2}{N}(S_1 - S_2)\right| \\ &\leq 2\left(\frac{\beta_1 S_1}{N}|A_1 - A_2| + \frac{\beta_1 A_2}{N}|S_1 - S_2| + \frac{\beta_2 S_1}{N}|I_1 - I_2|\right. \\ &\quad \left. + \frac{\beta_2 I_2}{N}|S_1 - S_2|\right), \end{aligned}$$

where

$$|S| \leq \frac{\Sigma}{N}, \quad |I| \leq \frac{\Sigma}{N} \quad \textit{and} \quad |A| \leq \frac{\Sigma}{N}.$$

Therefore,

$$\begin{aligned} |L(Y_1) - L(Y_2)| \leq & \frac{2\Sigma}{N}\left(\beta_1 |A_1 - A_2| + \beta_1 |S_1 - S_2| + \beta_2 |I_1 - I_2|\right. \\ & \left. + \beta_2 |S_1 - S_2|\right). \end{aligned}$$

By factoring out the common term, we obtain

$$\|\Theta(Y_1) - \Theta(Y_2)\| \leq \left(\frac{2\beta_1\Sigma}{N} + \frac{2\beta_2\Sigma}{N}\right)|S_1 - S_2| + \frac{2\beta_1\Sigma}{N}|A_1 - A_2|$$

$$
\begin{aligned}
&+ \frac{2\beta_2\Sigma}{N} |I_1 - I_2| \\
&\leq Z \|Y_1 - Y_2\|,
\end{aligned}
$$

where

$$
Z = \max\left(\frac{2\beta_1\Sigma}{N} + \frac{2\beta_2\Sigma}{N}, \frac{2\beta_1\Sigma}{N}, \frac{2\beta_2\Sigma}{N}, \|K\|\right).
$$

Therefore, it follows that the mapping L possesses the property of being uniformly Lipschitz continuous. In addition, by enforcing the conditions $S(t) \geq 0$, $V(t) \geq 0$, $E(t) \geq 0$, $I(t) \geq 0$, $A(t) \geq 0$, $H(t) \geq 0$, $R(t) \geq 0$, and $Q(t) \geq 0$ within the positive cone $\mathbb{R}^8_+$, we guarantee the existence of at least one solution to the proposed system. This ensures that all the state variables remain nonnegative for any admissible initial data, thereby validating the consistency of the model under the prescribed assumptions. Consequently, the system is mathematically well-posed, which provides a rigorous foundation for further qualitative and numerical investigations [40].

3 The control mathematical model

The control strategies in this model are focused on three main variables aimed at reducing disease transmission and mitigating its health impact. The variable $c_1(t)$ represents preventive interventions directed towards asymptomatic individuals (A), such as enhancing protective awareness, maintaining social distancing, wearing masks, and adopting hygienic practices that limit the hidden spread of infection from this group. The variable $c_2(t)$ is associated with symptomatic individuals (I), through their rapid isolation, provision of appropriate treatment, and reduction of direct contact with others, which significantly lowers the transmission rate. In contrast, the variable $c_3(t)$ refers to the strategy that allows infected individuals to choose to remain at home while adhering to prescribed medications. This reduces the burden on hospitals and contributes to containing the spread of the disease by minimizing community-level interactions.

The integration of these three strategies ensures a balance between prevention, treatment, and home isolation, thereby providing greater effectiveness in controlling the disease while minimizing the associated health and social costs.

Category 1: The combination of personal protection measures (c_1), vaccination (c_2), and awareness raising program (c_3): $c_1 \neq 0,\ c_2 \neq 0,\ c_3 \neq 0$.

Category 2: The combination of personal protection measures (u_1) and awareness raising program (c_3): $c_1 \neq 0,\ c_3 \neq 0$.

Category 3: The use of only vaccination (c_2): $c_2 \neq 0$.

Category 4: The combination of personal protection measures (c_1) and vaccination (c_2): $c_1 \neq 0,\ c_2 \neq 0$.

Therefore

$$\begin{cases} \frac{dS}{dt} = \Sigma(1-\alpha) - \beta_1 \frac{SA}{N}(1-c_1(t)) - \beta_2 \frac{SI}{N}(1-c_2(t)) - (k_1+\mu)S, \\ \frac{dV}{dt} = \Sigma\alpha + k_1 S + k_2 A - (\theta+\mu)V, \\ \frac{dE}{dt} = \beta_1 \frac{SA}{N}(1-c_1(t)) + \beta_2 \frac{SI}{N}(1-c_2(t)) - (\sigma+\mu)E, \\ \frac{dI}{dt} = \gamma\sigma E + dA - (\alpha_2 + n_1 + \varepsilon_1 + \mu)I, \\ \frac{dA}{dt} = (1-\gamma)\sigma E - (d + n_3 + \alpha_1 + \mu + k_2)A, \\ \frac{dH}{dt} = \alpha_1 A + \alpha_2 I - (\lambda+\mu)H, \\ \frac{dR}{dt} = \lambda H + n_3 A + n_2 Q + \theta V - \mu R + c_3(t)Q, \\ \frac{dQ}{dt} = n_1 I - (n_2 + \varepsilon_2 + \mu)Q - c_3(t)Q. \end{cases} \tag{2}$$

Given $(S(0) \geq 0, V(0) \geq 0, E(0) \geq 0, I(0) \geq 0, A(0) \geq 0, H(0) \geq 0, R(0) \geq 0,$
$Q(0) \geq 0) \in \mathbb{R}^8_+$, these are the prescribed initial conditions.

4 The challenge of finding the best control strategy

The central difficulty in this framework is the minimization of the objective functional [26, 36, 37, 38, 39], which necessitates achieving an appropriate compromise between the application of control strategies and the expenses they incur. The overarching aim is to construct an optimal control policy that reduces the functional to its lowest possible value, while simultaneously accounting for the efficiency of the interventions as well as their economic burden. More precisely, the objective functional $J(c_1, c_2, c_3)$ captures the balance between the prevalence of infection and the financial cost associated with implementing control actions. The epidemiological dynamics are described through the infected classes $I(t)$, $A(t)$, and $Q(t)$ together with the recovered class $R(t)$. On the other hand, the costs of interventions are represented by the control variables $c_1(t)$, $c_2(t)$, and $c_3(t)$, weighted by the positive constants k_1, k_2, and k_3, respectively. Consequently, the formulation provides a rigorous quantitative tool to evaluate different strategies and to determine the most effective approach in terms of both public health outcomes and resource allocation.

$$J(c_1, c_2, c_3) = I(T) + A(T) + Q(T) - R(T)$$

$$+\int_0^t \left(I(t) + A(t) + Q(t) - R(t) + \frac{k_1}{2}c_1^2(t) + \frac{k_2}{2}c_2^2(t) + \frac{k_3}{2}c_3^2(t) \right) dt.$$

The coefficients $k_1 \geq 0$, $k_2 \geq 0$ and $k_3 \geq 0$ are cost factors, chosen to balance the relative importance of $c_1(t)$, $c_2(t)$ and $c_3(t)$ at any time t, where $t_f = T$ represents the terminal time.

Our primary objective is to find the optimal controls c_1^*, c_2^* and c_3^* such that

$$J\left(c_1^*, c_2^*, c_3^*\right) = \min_{(c_1,c_2,c_3)\in U_{ad}} J\left(c_1, c_2, c_3\right). \tag{3}$$

where U_{ad} refers to the set of allowable controls, defined by the following constraints:

$$\begin{aligned} U_{ad} = \{c_1, c_2, c_3 | \, & 0 \leq c_{1\min} \leq c_1(t) \leq c_{1\max} \leq 1, \\ & 0 \leq c_{2\min} \leq c_2(t) \leq c_{2\max} \leq 1 \\ & 0 \leq c_{3\min} \leq c_3(t) \leq c_{3\max} \leq 1; \qquad t \in [0, t_f]\}. \end{aligned}$$

4.1 Existence of optimal control

Theorem 4. Consider the regulation problem for system (2). There exists an optimal control vector $(c_1^*(t), c_2^*(t), c_3^*(t)) \in U_{ad}$ such that

$$J(c_1^*(t), c_2^*(t), c_3^*(t)) = \min_{(c_1(t),c_2(t),c_3(t))\in U_{ad}} J(c_1(t), c_2(t), c_3(t)).$$

This holds under the following conditions:

1. The control set U_{ad} and the corresponding state variables are nonempty.

2. The system's right-hand side is bounded by a linear combination of the state and control variables.

3. The control set U_{ad} is both convex and closed.

4. The integral $M(S, E, A, I, V, H, R, Q, c_1, c_2, c_3)$ within the objective function is convex over the admissible control set U_{ad}.

Proof. **Condition 1.**

To prove the nonemptiness of the control set and the associated state variables, we employ an existence theorem from Boyce et al. [12].

Consider the system described by $\dot{Y}_i = Y_{K_i}(t, Y_1, Y_2, Y_3, Y_4, Y_5, Y_6, Y_7, Y_8)$ for $i \in \{1, \ldots, 8\}$, where $(Y_1, Y_2, Y_3, Y_4, Y_5, Y_6, Y_7, Y_8) = (S, E, A, I, V, H, R, Q)$. The functions $Y_S, Y_E, Y_A, Y_I, Y_V, Y_H, Y_R$ and Y_Q represent the right-hand side of (3). Given that all parameters are constants and $Y_1, Y_2, Y_3, Y_4, Y_5, Y_6, Y_7$ and Y_8 are continuous functions, it follows that $Y_S, Y_E, Y_A, Y_I, Y_V, Y_H, Y_R$ and Y_Q are also continuous. Additionally, the partial derivatives $\frac{\partial Y_{Y_i}}{\partial Y_i}$ for $i \in \{1, \ldots, 8\}$ are continuous.

Thus, a unique solution (S, E, A, I, V, H, R, Q) exists that satisfies the initial conditions, indicating that the control set and the corresponding state variables are nonempty, thus meeting the first condition.

Condition 2.

By definition, the admissible control set U_{ad} is closed. Consider any controls $(c_1, c_2, c_3) \in U_{ad}$ and $\xi \in [0, 1]$. We need to demonstrate that $0 \leq \xi c_1 + (1 - \xi)c_3 \leq 1$. Indeed, it follows that $\xi c_1 \leq \xi$ and $(1 - \xi)c_3 \leq (1 - \xi)$, which implies that $\xi c_1 + (1 - \xi)c_3 \leq \xi + (1 - \xi) = 1$. Therefore, we have $0 \leq \xi c_1 + (1 - \xi)c_3 \leq 1$ for all $(c_1, c_2, c_3) \in U_{ad}$ and $\xi \in [0, 1]$. This confirms that U_{ad} is both closed and convex, thereby satisfying the second condition.

Condition 3.

The right-hand sides of system (2) are continuous and bounded by a linear combination of the state variables and control inputs. Furthermore, they can be expressed as a linear function in terms of c_1, c_2 and c_3, with coefficients that depend on both the state variables and time.

Condition 4.

The integral within the objective function $I(t)+A(t)+Q(t)-R(t)+\frac{k_1}{2}c_1^2(t)+\frac{k_2}{2}c_2^2(t)+\frac{k_3}{2}c_3^2(t)$ is inherently convex over the set U_{ad}. Indeed, there exist constants Φ_1 and Φ_2, with $\beta > 1$, such that the integral in the objective functional satisfies

$$M(S, E, A, I, V, H, R, Q, c_1, c_2, c_3) \geq \Phi_1 + \Phi_2(|c_1|^2 + |c_2|^2 + |c_3|^2)^{\frac{\kappa}{2}},$$

where

$$\begin{aligned} &I(t) + A(t) + Q(t) - R(t) + \frac{k_1}{2}c_1^2(t) + \frac{k_2}{2}c_2^2(t) + \frac{k_3}{2}c_3^2(t) \\ &\quad \geq \Phi_1 + \Phi_2(|c_1|^2 + |c_2|^2 + |c_3|^2)^{\frac{\kappa}{2}}. \end{aligned}$$

Given that the state variables are bounded, let

$$\begin{aligned} \Phi_1 &= 4 \inf_{t \in [0,T]} (I(t) + A(t) + Q(t) - R(t)), \\ \Phi_2 &= \inf\left(\frac{k_1}{2}, \frac{k_2}{2}, \frac{k_3}{2}\right), \quad \textit{and} \quad \kappa = 2. \end{aligned}$$

□

Therefore, following the results presented by Fleming and Richel [19], and further elaborated in [35, 42, 43], we can confirm the existence of an optimal control.

4.2 Characterization of optimal control

In this part of the study, Pontryagin's maximum principle [37] is employed as a fundamental analytical framework for addressing the optimal control problem. The methodology begins with the introduction of the adjoint variables, which serve as an essential mathematical link between the system of differential equations describing the dynamics and the objective functional targeted for optimization. This relationship naturally leads to the construction of the Hamiltonian function, a central quantity that integrates both the system dynamics and the objectives of the control process.

By invoking Pontryagin's principle, the challenging task of determining an optimal control policy under given initial conditions is reformulated into the problem of continuously optimizing the Hamiltonian over time. This transformation not only simplifies the search for the optimal solution but also provides a systematic procedure to guide the system toward the desired outcome. Furthermore, this approach establishes a solid theoretical basis for exploring qualitative properties of the solutions and for developing efficient numerical algorithms capable of implementing the optimal strategies in practice.

We now define the Hamiltonian H at a given time t as follows:

$$\begin{aligned} H = I(t) + A(t) + Q(t) - R(t) + \frac{k_1}{2}c_1^2(t) + \frac{k_2}{2}c_2^2(t) + \frac{k_3}{2}c_3^2(t) \\ + \sum_{i=1}^{8} \psi_i(t)\, u_i(S, E, A, I, V, H, R, Q). \end{aligned}$$

In this scenario, u_i denotes the right-hand side of the differential equations system (2) for the i-th state variable, and ψ_i represents the corresponding adjoint functions. These adjoint functions are linked to the state variables and are used to reflect the impact of changes in the state on the cost functional.

Theorem 5. Suppose that $(c_1^*, c_2^*, c_3^*) \in U_{ad}$ denotes the optimal control variables, and let S^*, E^*, A^*, I^*, V^*, H^*, R^*, and Q^* represent the corresponding optimal trajectories for the state variables. Then, there exist adjoint functions ψ_1, ψ_2, ψ_3, ψ_4, ψ_5, ψ_6, ψ_7 and ψ_8 that satisfy the following conditions:

$$
\begin{aligned}
\psi_1' &= -\frac{\partial H}{\partial S} = \left(\beta_1 \frac{A}{N}(1-c_1) + \beta_2 \frac{I}{N}(1-c_2)\right)(\psi_1 - \psi_3) \\
&\quad + k_1(\psi_1 - \psi_2) + \mu\psi_1, \\
\psi_2' &= -\frac{\partial H}{\partial V} = \theta(\psi_2 - \psi_7) + \mu\psi_2, \\
\psi_3' &= -\frac{\partial H}{\partial E} = \sigma(\psi_3 - \psi_5) + \gamma\sigma(\psi_5 - \psi_4) + \mu\psi_3, \\
\psi_4' &= -\frac{\partial H}{\partial I} = -1 + \frac{\beta_2 S}{N}(1-c_2)(\psi_1 - \psi_3) \\
&\quad + \alpha_2(\psi_4 - \psi_6) + n_1(\psi_4 - \psi_8) + (\mu + \varepsilon_1)\psi_4, \\
\psi_5' &= -\frac{\partial H}{\partial A} = -1 + \frac{\beta_1 S}{N}(1-c_1)(\psi_1 - \psi_3) \\
&\quad + d(\psi_5 - \psi_4) + n_3(\psi_5 - \psi_7) + \alpha_1(\psi_5 - \psi_6) \\
&\quad + k_2(\psi_5 - \psi_2) + \mu\psi_5, \\
\psi_6' &= -\frac{\partial H}{\partial H} = \lambda(\psi_6 - \psi_7) + \mu\psi_6, \\
\psi_7' &= -\frac{\partial H}{\partial R} = 1 + \mu\psi_7, \\
\psi_8' &= -\frac{\partial H}{\partial Q} = -1 + (\psi_8 - \psi_7)(n_2 + c_3) + (\mu + \varepsilon_2)\psi_8.
\end{aligned}
$$

With the transversality conditions, ψ_1, ψ_2, ψ_5, and ψ_7 are all equal to zero at time T. On the other hand, ψ_3, ψ_4, and ψ_8 are set to minus one, and ψ_6 is set to one at the same time point.

The solution to the optimal control problem is provided by the control variables c_1^*, c_2^* and c_3^*. The optimal control values are obtained as follows:

$$
\begin{cases}
c_1^* = \min\left(1, \max\left(0, \frac{\beta_1 SA(\psi_3 - \psi_1)}{k_1 N}\right)\right), \\
c_2^* = \min\left(1, \max\left(0, \frac{\beta_2 SI(\psi_3 - \psi_1)}{k_2 N}\right)\right), \\
c_3^* = \min\left(1, \max\left(0, \frac{Q(\psi_8 - \psi_7)}{k_3}\right)\right).
\end{cases} \tag{4}
$$

Proof. The Hamiltonian H at any time t can be represented as follows:

$$
\begin{aligned}
H =& I(t) + A(t) + Q(t) - R(t) + \frac{k_1}{2}c_1^2(t) + \frac{k_2}{2}c_2^2(t) + \frac{k_3}{2}c_3^2(t) \\
&+ \psi_1 \left\{ \Sigma(1-\alpha) - \beta_1 \frac{S(t)A(t)}{N}(1 - c_1(t)) \right. \\
&\left. - \beta_2 \frac{S(t)I(t)}{N}(1 - c_2(t)) - (k_1 + \mu)S(t) \right\} \\
&+ \psi_2 \left\{ \Sigma\alpha + k_1 S(t) + k_2 A(t) - (\theta + \mu)V(t) \right\}
\end{aligned}
$$

$$
\begin{aligned}
&+ \psi_3 \left\{ \beta_1 \frac{S(t)A(t)}{N} \left(1 - c_1(t)\right) + \beta_2 \frac{S(t)I(t)}{N} \left(1 - c_2(t)\right) - (\sigma + \mu)E(t) \right\} \\
&+ \psi_4 \left\{ \gamma\sigma E(t) + dA(t) - (\alpha_2 + n_1 + \varepsilon_1 + \mu)I(t) \right\} \\
&+ \psi_5 \left\{ (1-\gamma)\sigma E(t) - (d + n_3 + \alpha_1 + \mu + k_2)A(t) \right\} \\
&+ \psi_6 \left\{ \alpha_1 A(t) + \alpha_2 I(t) - (\lambda + \mu)H(t) \right\} \\
&+ \psi_7 \left\{ \lambda H(t) + n_3 A(t) + n_2 Q(t) + \theta V(t) - \mu R(t) + c_3(t)Q(t) \right\} \\
&+ \psi_8 \left\{ n_1 I(t) - (n_2 + \varepsilon_2 + \mu)Q(t) - c_3(t)Q(t) \right\}.
\end{aligned}
$$

Using Pontryagin's maximum principle [27], we derived the adjoint equations and the transversality conditions, which are expressed as follows:

$$\psi_i{}' = -\tfrac{\partial H}{\partial Y_i} \text{ and } \psi_i(t_f) = 0 \text{ for } i \in \{1, 2, 5, 7, 8\},$$

where $(Y_1, Y_2, Y_3, Y_4, Y_5, Y_6, Y_7, Y_8) = (S, E, A, I, V, H, R, Q)$.

The transversality conditions require that, at the terminal time, the adjoint variables must satisfy an orthogonality relation with the attainable set of the final state. This condition plays a crucial role in guaranteeing the mathematical consistency of the optimal control formulation and ensures that the resulting solution is both coherent and reliable. By enforcing these requirements, one can explicitly characterize the optimal control functions, denoted by $c_1^*(t)$, $c_2^*(t)$, and $c_3^*(t)$, for the entire time horizon $t \in [0, t_f]$. Such conditions not only facilitate the identification of the most effective control strategies but also provide a rigorous framework that enhances the interpretability of the results and supports the implementation of optimal policies in practical scenarios.

$$\frac{\partial H}{\partial c_1} = 0, \qquad \frac{\partial H}{\partial c_2} = 0 \qquad \textit{and} \qquad \frac{\partial H}{\partial c_3} = 0.$$

Consequently,

$$
\begin{aligned}
\frac{\partial H}{\partial c_1} &= k_1 c_1 + \psi_1 \beta_1 \frac{SA}{N} - \psi_3 \beta_1 \frac{SA}{N} = 0, \\
\frac{\partial H}{\partial c_2} &= k_2 c_2 + \psi_1 \beta_2 \frac{SI}{N} - \psi_3 \beta_2 \frac{SI}{N} = 0, \\
\frac{\partial H}{\partial c_3} &= k_3 c_3 + \psi_7 Q - \psi_8 Q = 0.
\end{aligned}
$$

Therefore,

$$c_1^* = \frac{\beta_1 SA(\psi_3 - \psi_1)}{k_1 N},$$

$$c_2^* = \frac{\beta_2 SI(\psi_3 - \psi_1)}{k_2 N},$$
$$c_3^* = \frac{Q(\psi_8 - \psi_7)}{k_3}.$$

Given the constraints within U_{ad} for the control variables, we can efficiently determine the optimal controls c_1^*, c_2^* and c_3^* as expressed in (4). □

5 Numerical simulation

In this section, we focus on the numerical simulation of the proposed optimal control problem, which is carried out by applying the well-known Forward-Backward Sweep method [45]. The approach consists of integrating the state system (1) forward in time while simultaneously solving the corresponding adjoint system backward in time. The two procedures are repeated in an iterative manner, with updated values of the control functions at each step. This forward-backward process continues until the solutions converge to an optimal trajectory. Once a satisfactory level of convergence between the state and adjoint systems is achieved, the iterative procedure is terminated. The results obtained from this algorithm are then illustrated and analyzed graphically to highlight the effectiveness of the derived control strategies.

In this study, the parameter values presented in Table 1 were selected under hypothetical assumptions, since real epidemiological data were not available. This choice allowed us to design and analyze the model even in the absence of empirical evidence. The use of assumed parameter values provided the flexibility to examine different possible trajectories and disease dynamics that could emerge from the system. Such an approach makes it possible to conduct an in-depth investigation of the model's performance under diverse scenarios, while also laying the groundwork for future validation once reliable data become accessible. Furthermore, adopting hypothetical scenarios serves to highlight potential weaknesses in the model and to point out directions where additional research is needed, thereby ensuring that the framework remains sufficiently robust and adaptable to multiple contexts. The simulated values employed in this model were specifically chosen to conduct a theoretical investigation of the potential impacts of personal protective measures, vaccination, and awareness programs on reducing the spread of meningitis. It is important to emphasize that this constitutes a purely theoretical analysis, intended to capture the possible outcomes under different intervention strategies rather than relying on real-world data. Furthermore, based on assumptions related to the prevention of meningitis, the three control variables, denoted here as c_1, c_2 and c_3, are constrained within given intervals. These constraints reflect the realistic limits of implementing such interventions

Table 1: Details on the parameters involved in the meningitis modeling.

Parameter	**Values in d^{-l}**	**Reference**	**Parameter**	**Values in d^{-l}**	**Reference**
μ	3.933×10^{-5}	[31]	θ	0.41	Assumed
β_1	0.476	Estimated	σ	0.4	[32]
β_2	0.238	Estimated	Σ	9.43×10^5	[31]
α	0.19	[32]	γ	0.63	[32]
λ	0.88	[34]	n_1	0.0013	Simulated
d	0.0013	[34]	n_2	0.0015	Simulated
k_1	0.2	[33]	n_3	0.017	Simulated
k_2	0.1	[33]	ϵ_1	0.017	Simulated
α_1	0.023	Assumed	ϵ_2	0.012	Simulated
α_2	0.045	Assumed			

in practice, where the level of adoption cannot exceed certain thresholds but also cannot be entirely absent. In the subsequent part of this study, we classify the possible intervention strategies into four distinct categories. Each category represents a particular combination of control measures, and together they serve as the foundation for evaluating the effectiveness of optimal control strategies in mitigating the dynamics of meningitis transmission.

Category 1: The combination of personal protective measures for asymptomatic individuals (c_1), interventions targeting symptomatic individuals (c_2), and quarantine and screening strategies (c_3): $c_1 \neq 0,\ c_2 \neq 0,\ c_3 \neq 0$.

Category 2: The combination of personal protective measures for asymptomatic individuals (c_1) and quarantine and screening strategies (c_3): $c_1 \neq 0,\ c_3 \neq 0$.

Category 3: The use of only interventions targeting symptomatic individuals (c_2): $c_2 \neq 0$.

Category 4: The combination of personal protective measures for asymptomatic individuals (c_1) and interventions targeting symptomatic individuals (c_2): $c_1 \neq 0,\ c_2 \neq 0$.

5.1 Strategy 1: This case involves the combined implementation of personal protection measures (c_1), vaccination (c_2), and awareness-raising programs (c_3), where $c_1 \neq 0,\ c_2 \neq 0,\ c_3 \neq 0$

It can therefore be concluded that when optimal control strategies are applied, namely personal protective measures (c_1), vaccination (c_2), and awareness-raising programs (c_3), epidemic outbreaks do not occur. Figure 2 provides a complete illustration of how these control interventions are implemented in the model. Subfigures 2(a), 2(b), 2(c), and 2(d) display the temporal dynamics of the infected (I), asymptomatic infected (A), exposed (E), and recovered (R) populations under Category 1. A key feature of this category is the significant increase in the proportion of recoverers in the population. In particular, Figure 2(d) shows that the proportion of recovered individuals rises to nearly 0.6, indicating that more than half of the population has effectively achieved immunity. Furthermore, Figure 2(e) illustrates the temporal trajectories of the control functions c_1, c_2 and c_3. It can be observed that these controls are maintained at their maximum levels for approximately the first 155, 154, and 80 days, respectively, after which they gradually decline in a monotonic manner toward their minimum values. This behavior reflects the intensive initial interventions needed to curb transmission, followed by a progressive relaxation of measures once the epidemic is under control.

5.2 Strategy 2: This scenario considers the joint implementation of personal protection measures (c_1) together with awareness-raising programs (c_3), where both $c_1 \neq 0$ and $c_3 \neq 0$

In this category, Figure 3 presents the simulation outcomes of applying the control strategies associated with Category 2, namely the combination of personal protection measures (c_1) and awareness programs (c_3). Subfigures 2(a)–2(b) illustrate the trajectories of symptomatic infections, asymptomatic infections, and exposed individuals, respectively. In each case, the number of infected individuals is consistently lower when the controls are implemented compared to the uncontrolled scenario. This demonstrates the effectiveness of preventive awareness and personal

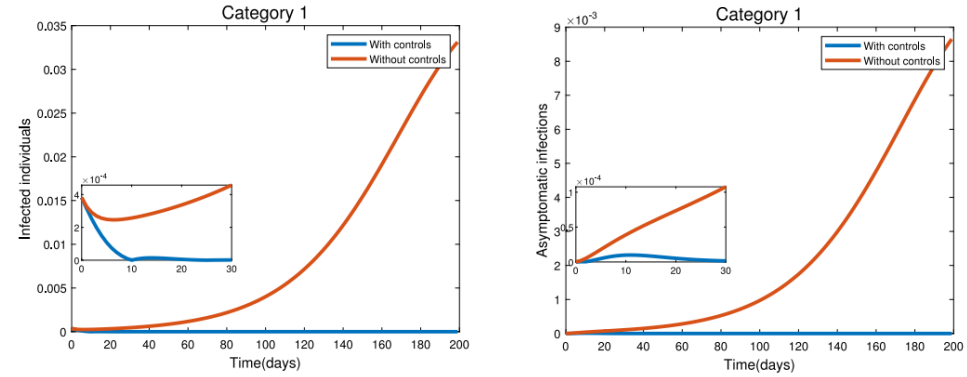

(a)

(b)

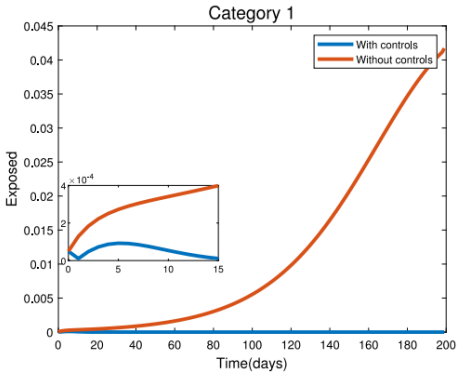

(c)

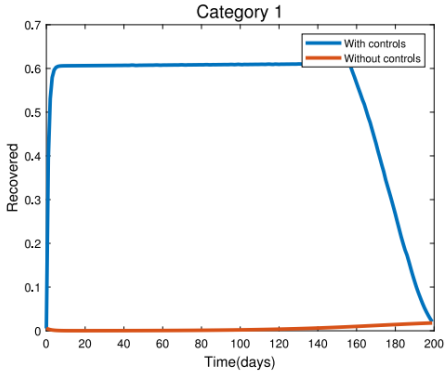

(d)

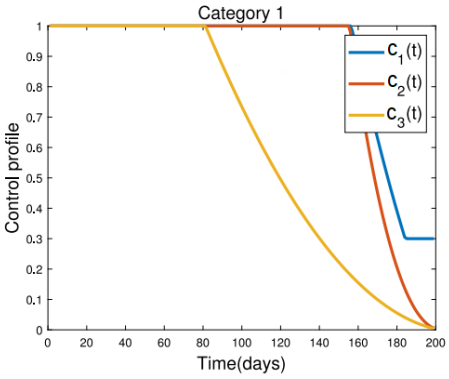

(e)

Figure 2: Numerical results for Category 1. Figures (a), (b), (c), and (d) illustrate the dynamics of symptomatic cases, asymptomatic cases, exposed individuals, and recovered individuals, respectively. Figure (e) displays the trajectories of the optimal control variables.

protection in reducing the rate of new infections and slowing the overall spread of the disease. Figure 2(d) shows that, under Category 2, the number of recovered individuals drops to zero after approximately ten days and remains at zero for the rest of the simulation period. This implies that in the absence of vaccination, no recoverers will exist within the population, which highlights the crucial role of vaccination in sustaining immunity.

Overall, these results indicate that Category 2 can significantly suppress the infection dynamics through awareness and protection alone, but without vaccination, recovery is not achieved, leaving the population vulnerable to future waves of infection.

5.3 Strategy 3: Vaccination as the sole intervention (c_2) where $c_2 \neq 0$

This category greatly increases the proportion of recoverers in the population; as shown in Figure 4(d), the proportion is as high as 0.6. In Figure 4(e) depicts controls c_1, c_2 and c_3, which govern the system over the simulation horizon.

5.4 Strategy 4: The joint application of personal protection measures (c_1) and vaccination (c_2) where $c_1 \neq 0$ and $c_2 \neq 0$

Figure 5 depicts the scenario in which the controls c_1 and c_2 are applied to system (1). Under this category, the proportion of recoverers in the population rises substantially, reaching as high as 0.6 as indicated in Figure 5(d).

Discussion

Figure 6 illustrates the dynamics of the different population compartments in system (1), derived from simulations of the four optimal control categories. Nevertheless, the effectiveness of these categories varies. Although many individuals recognize that meningitis is highly contagious and transmitted through multiple routes, some still neglect preventive practices and refrain from participating in vaccination programs. This behavior hinders the potential for a substantial

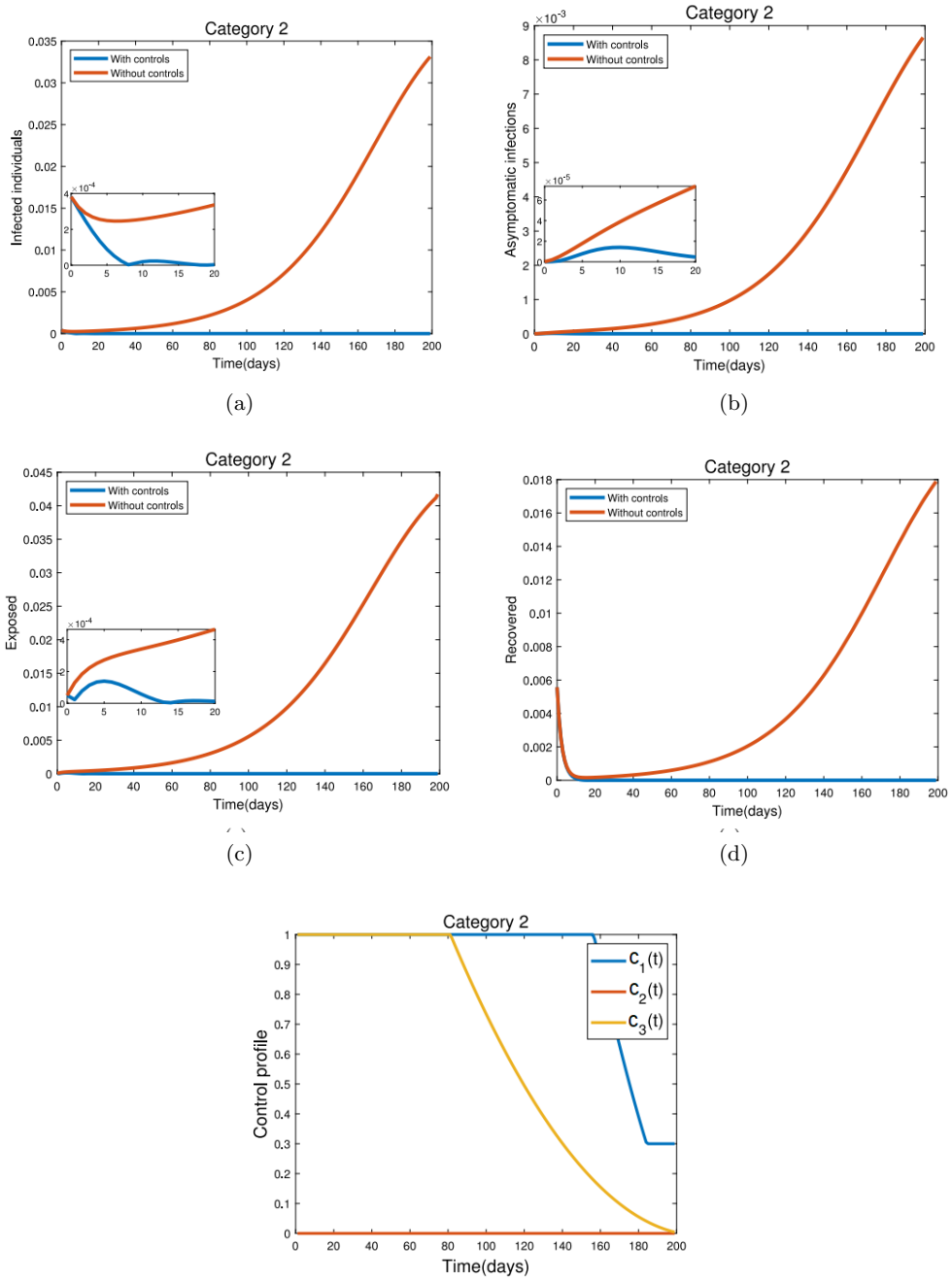

Figure 3: Numerical results for Category 2. Figures (a), (b), (c), and (d) illustrate the dynamics of symptomatic cases, asymptomatic cases, exposed individuals, and recovered individuals, respectively. Figure (e) displays the trajectories of the optimal control variables.

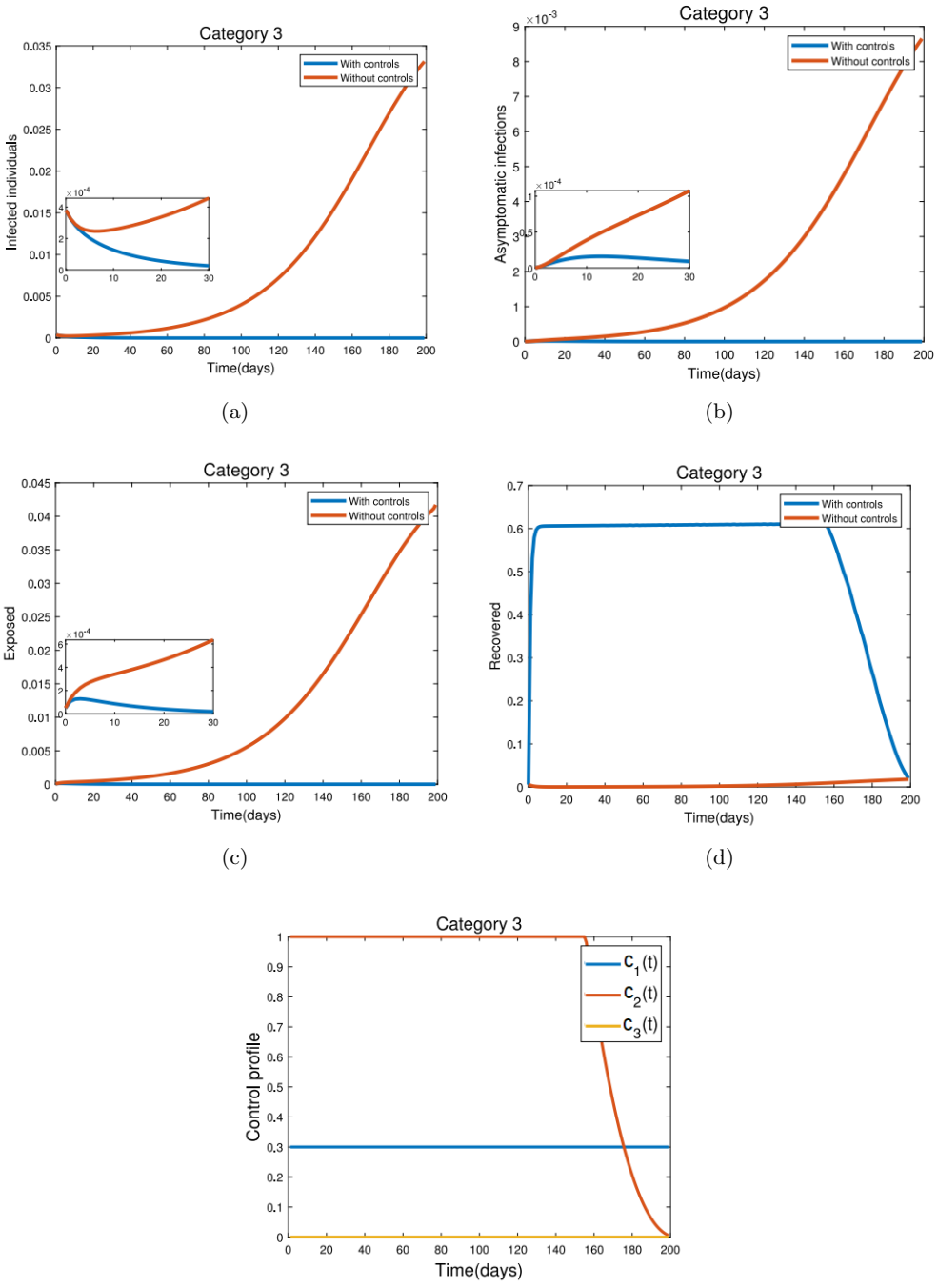

Figure 4: Numerical results for Category 3. Figures (a), (b), (c), and (d) illustrate the dynamics of symptomatic cases, asymptomatic cases, exposed individuals, and recovered individuals, respectively. Figure (e) displays the trajectories of the optimal control variables.

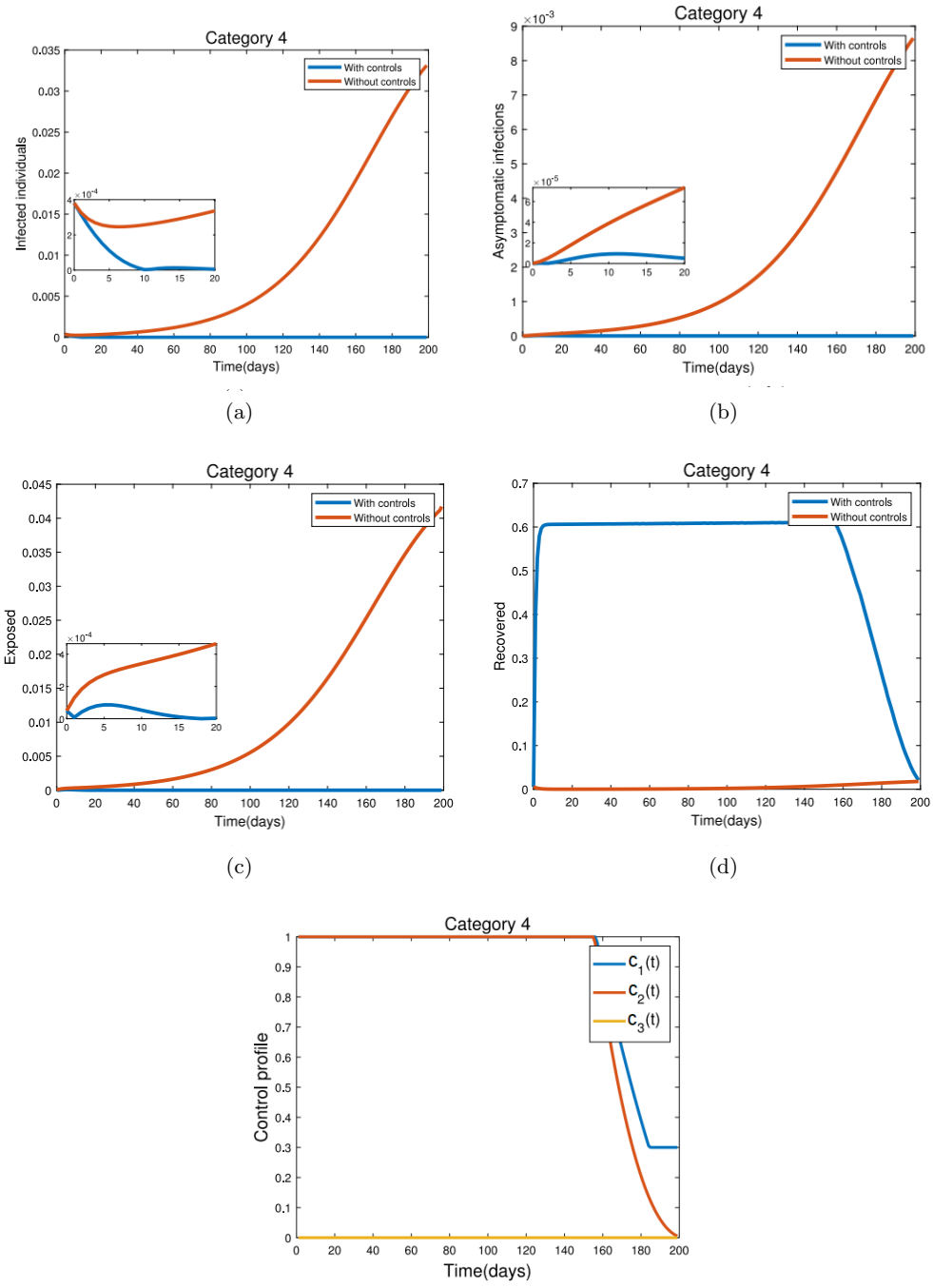

Figure 5: Numerical results for Category 4. Figures (a), (b), (c), and (d) illustrate the dynamics of symptomatic cases, asymptomatic cases, exposed individuals, and recovered individuals, respectively. Figure (e) displays the trajectories of the optimal control variables.

reduction in meningitis cases. Among the interventions, the adoption of control strategy c_2 (vaccination) plays a critical role in increasing the number of recoverers within the population. In the absence of vaccination, no immune individuals would emerge, and the entire population would remain susceptible, thereby elevating the risk of disease.

Moreover, the application of control measures c_1 and c_3 helps to strengthen public awareness and protective behavior. Collectively, the four categories of control strategies are shown to decrease the number of infections while simultaneously enlarging the recovered population. These findings suggest that vaccination and awareness-raising interventions should be promoted more vigorously, as they effectively lower infection rates and, in turn, reduce disease risks.

The analysis further reveals that while individual control measures are beneficial, combining two interventions yields greater effectiveness compared to applying them separately. More importantly, the simultaneous implementation of all three measures achieves the highest level of control, resulting in the fewest infections and the greatest number of recoveries. Overall, the results confirm that the strategic use of these optimal controls can markedly reduce the burden of infection. With adequate prevention and sustained control measures in place, the epidemic situation can be stabilized, allowing individuals to return to normal life.

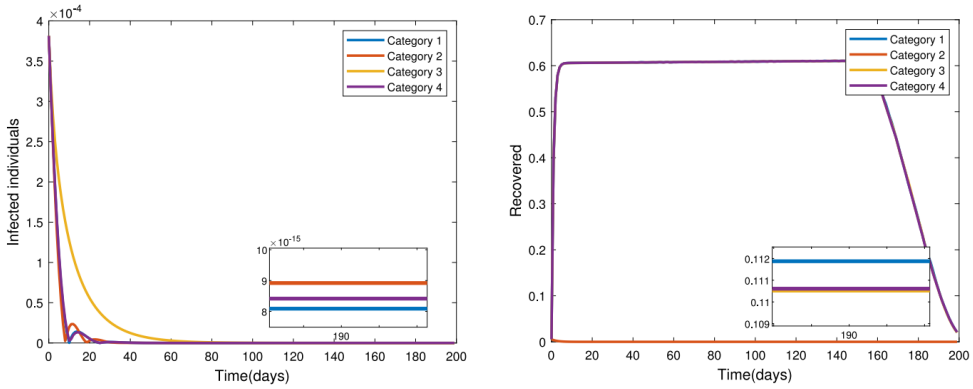

(a) (b)

Figure 6: Dynamics of the different population groups in system (1), as generated through simulations under the four optimal control strategies.

6 Conclusion

In this work, we developed and analyzed a comprehensive $SEAIVHRQ$ mathematical model for the transmission dynamics and control of meningitis. By integrating medical and behav-

ioral factors such as vaccination, hospitalization, and voluntary quarantine, the model provides a more realistic description of disease spread, particularly in regions with limited healthcare resources. The incorporation of three time-dependent control variables—reducing transmission from asymptomatic and symptomatic individuals, and promoting awareness and treatment adherence—allowed us to formulate an optimal control problem solved via Pontryagin's maximum principle.

Numerical simulations demonstrated that combining preventive, treatment, and awareness interventions can significantly lower infection peaks, reduce hospitalization demand, and minimize total costs. These results emphasize that a coordinated and sustained public health response is essential to achieving effective epidemic mitigation.

Overall, the proposed framework contributes a novel tool for understanding and managing meningitis epidemics, aligning with the WHO's roadmap "Defeating Meningitis by 2030". Future extensions may consider stochastic effects, fractional-order dynamics, and spatial heterogeneity to further enhance model realism and applicability to real-world health policy planning.

Funding

This research received no external funding.

Conflicts of Interest

The authors declare no conflicts of interest.

References

[1] Agusto, F.B., and Leite, M.C.A., *Optimal control and cost-effective analysis of the 2017 meningitis outbreak in Nigeria*, Infect. Dis. Model. 4 (2019), 161–187.

[2] Ali, S.A., Taj, M.K., and Ali, S.H., *Antimicrobial resistance pattern of bacterial meningitis among patients in Quetta, Pakistan*, Infect. Drug Resist. 14 (2021), 5107–5120.

[3] Asamoah, J.K.K., Nyabadza, F., Jin, Z., Bonyah, E., Khan, M.A., Li, M.Y., and Hayat, T., *Backward bifurcation and sensitivity analysis for bacterial meningitis transmission dynamics with a nonlinear recovery rate*, Chaos Solitons Fractals 140 (2020), Article 110237.

[4] Asamoah, J.K.K., Nyabadza, F., Seidu, B., Chand, M., and Dutta, H., *Mathematical modelling of bacterial meningitis transmission dynamics with control measures*, Comput. Math. Methods Med. 2018 (2018), Article ID 2657461.

[5] Ashchepkov, L.T., Dolgy, D.V., Kim, T., and Agarwal, R.P., *General optimal control problem*, In *Optimal Control*, Springer, Cham, 2021.

[6] Baroudi, M., Gourram, H., Alia, M., Labzai, A., and Belam, M., *Mathematical modeling and optimal control approaches for dengue*, Iran. J. Numer. Anal. Optim. 15(1) (2025), 396–423.

[7] Baroudi, M., Smouni, I., Gourram, H., Labzai, A., and Belam, M., *Advanced mathematical modeling and prognostication of regulated spatio-temporal dynamics of monkeypox*, Iran. J. Numer. Anal. Optim. 14(4) (2024) 1280–1308.

[8] Baroudi, M., Smouni, I., Gourram, H., Labzai, A., and Belam, M., *Optimizing control strategies for monkeypox through mathematical modeling*, Partial Differ. Equ. Appl. Math. 12 (2024), Article 100996.

[9] Belay, M.A., Abonyo, O.J., and Theuri, D.M., *Mathematical model analysis for the transmission dynamics of bacterial meningitis disease incorporating drug-resistance class*, Commun. Math. Biol. Neurosci. 2022 (2022), Article ID 121.

[10] Belay, M.A., Abonyo, O.J., and Theuri, D.M., *Mathematical model of hepatitis B disease with optimal control and cost-effectiveness analysis*, Comput. Math. Methods Med. 2023 (2023), Article ID 5215494.

[11] Bowong, S., and Kurths, J., *Modelling tuberculosis and hepatitis B co-infections*, Math. Model. Nat. Phenom. 5(6) (2010), 196–242.

[12] Boyce, W.E., DiPrima, R.C., and Meade, D.B., *Elementary differential equations*, John Wiley & Sons, Hoboken, NJ, 2017.

[13] Brozak, S.J., Pant, B., Safdar, S., and Gumel, A.B., *Dynamics of COVID-19 pandemic in India and Pakistan: a metapopulation modelling approach*, Infect. Dis. Model. 6 (2021), 1173–1201.

[14] Castillo-Chavez, C., and Song, B., *Dynamical models of tuberculosis and their applications*, Math. Biosci. Eng. 1(2) (2004), 361–404.

[15] Chandani, S., Jani, D., Sahu, P.K., Kataria, U., Suryawanshi, S., Khubchandani, J., Thorat, S., Chitlange, S. and Sharma, D. *COVID-19 vaccination hesitancy in India: state of the nation and priorities for research*, Brain Behav. Immun. Health 18 (2021), 100375.

[16] Cui, J., Lv, J., and Guo, S., *Dynamical model of emerging infectious diseases applied to COVID-19 transmission*, Acta Math. Appl. Sin. 43 (2020), 147–155.

[17] Donovan, C., and Blewitt, J., *Signs, symptoms and management of bacterial meningitis*, Nurs. Child. Young People 22(9) (2010).

[18] Epidemiology Working Group for NCIP Epidemic Response, Chinese Center for Disease Control and Prevention *The epidemiological characteristics of an outbreak of 2019 novel coronavirus diseases (COVID-19) in China*, Chin. J. Epidemiol. 41 (2020), 145–151.

[19] Fleming, W.H., and Rishel, R.W., *Deterministic and stochastic optimal control*, Vol. 1, Springer, New York, 2012.

[20] Gourram, H., Sahib, I., Baroudi, M., Smouni, I., Labzai, A., and Belam, M., *Analysis of the stability of a mathematical model for measles*, Commun. Math. Biol. Neurosci. 2025 (2025), Article ID 55.

[21] Irving, T.J., Blyuss, K.B., Colijn, C., and Trotter, C.L., *Modelling meningococcal meningitis in the African meningitis belt*, Epidemiol. Infect. 140(5) (2012), 897–905.

[22] Khajanchi, S., *Stability analysis of a mathematical model for glioma–immune interaction under optimal therapy*, Int. J. Nonlinear Sci. Numer. Simul. 20(3–4) (2019), 269–285.

[23] Khajanchi, S., and Banerjee, S., *A strategy of optimal efficacy of T11 target structure in the treatment of brain tumor*, J. Biol. Syst. 27(2) (2019), 225–255.

[24] Khajanchi, S., and Ghosh, D., *The combined effects of optimal control in cancer remission*, Appl. Math. Comput. 271 (2015), 375–388.

[25] Khan, M.A., Islam, S., Arif, M., and ul Haq, Z., *Transmission model of hepatitis B virus with the migration effect*, BioMed Res. Int. 2013 (2013), Article ID 150681.

[26] Kinfe, H., Sendo, E.G., and Gebremedhin, K.B., *Prevalence of hepatitis B virus infection and factors associated with hepatitis B virus infection among pregnant women presented to antenatal care clinics at Adigrat General Hospital in Northern Ethiopia*, Int. J. Women's Health 13 (2021), 119–127.

[27] Lenhart, S., and Workman, J.T., *Optimal control applied to biological models*, Chapman & Hall/CRC, Boca Raton, FL, 2007.

[28] Martcheva, M., and Crispino-O'Connell, G., *The transmission of meningococcal infection: a mathematical study*, J. Math. Anal. Appl. 283(1) (2003), 251–275.

[29] Maseno, K., *Mathematical model for malaria and meningitis co-infection among children*, Appl. Math. Sci. 5(47) (2011), 2337–2359.

[30] Mazamay, S., Guégan, J.-F., Diallo, N., Bompangue, D., Bokabo, E., Muyembe, J.-J., Taty, N., Vita, T.P., and Broutin, H., *An overview of bacterial meningitis epidemics in Africa from 1928 to 2018 with a focus on epidemics "outside-the-belt"*, BMC Infect. Dis. 21(1) (2021), Article 1027.

[31] McCarthy, J.J., *A thematic guide to optimality theory*, Cambridge Univ. Press, Cambridge, 2002.

[32] Misra, A.K., Singh, R.K., Tiwari, P.K., Khajanchi, S., and Kang, Y., *Dynamics of algae blooming: effects of budget allocation and time delay*, Nonlinear Dyn. 100(2) (2020), 1779–1807.

[33] Mo, X., Xu, X., Ren, Z., Guan, J., and Peng, J., *Patients with tuberculous meningitis and hepatitis B co-infection have increased risk for antituberculosis drug-induced liver injury and poor outcomes*, Infect. Dis. 52(11) (2020), 793–800.

[34] Mondal, J., Khajanchi, S., and Akhtar, M.N., *A mathematical model for COVID-19 pandemic with the impact of economic development*, In *Fractal signatures in the dynamics of an epidemiology*, CRC Press, Boca Raton, FL, 2023.

[35] Nandi, S., Khajanchi, S., Chatterjee, A.N., and Roy, P.K., *Insight of viral infection of Jatropha curcas plant (Future Fuel): a control-based mathematical study*, Acta Analysis Functionalis Applicata 13(04) (2011), 366–374.

[36] Olaniyi, S., Ajala, O.A., and Abimbade, S.F., *Optimal control analysis of a mathematical model for recurrent malaria dynamics*, Oper. Res. Forum vol. 4, no. 1, p. 14. Cham: Springer International Publishing, 2023.

[37] Pontryagin, L.S., *Mathematical theory of optimal processes*, CRC Press, Boca Raton, FL, 1987.

[38] Sahib, I., Baroudi, M., Gourram, H., Khajji, B., Labzai, A., and Belam, M., *The mathematical modeling and analysis of the cholera disease model*, Commun. Math. Biol. Neurosci. 2024 (2024), Article ID 93.

[39] Shen, W.-Y., Chu, Y.-M., Rahman, M.U., Mahariq, I., and Zeb, A., *Mathematical analysis of HBV and HCV co-infection model under nonsingular fractional order derivative*, Results Phys. 28 (2021), Article 104582.

[40] Smouni, I., Baroudi, M., Alia, M., Elmansouri, A., Labzai, A., and Belam, M., *Spatiotemporal stability analysis of soil-borne disease dynamics in tomato plants*, Model. Earth Syst. Environ. 11(2) (2025), Article 105.

[41] Spearman, C.W., Afihene, M., Ally, R., Apica, B., Awuku, Y., Cunha, L., Dusheiko, G., Gogela, N., Kassianides, C., and Kew, M., *Hepatitis B in sub-Saharan Africa: strategies to achieve the 2030 elimination targets*, Lancet Gastroenterol. Hepatol. 2(12) (2017), 900–909.

[42] Tilahun, G.T., *Optimal control analysis of pneumonia and meningitis coinfection*, Comput. Math. Methods Med. 2019 (2019), Article ID 2658971.

[43] World Health Organization, *Hepatitis B*, WHO/CDS/CSR/LYO/2002.2, World Health Organization, Geneva, 2002.

[44] Zhao, S., Xu, Z., and Lu, Y., *A mathematical model of hepatitis B virus transmission and its application for vaccination strategy in China*, Int. J. Epidemiol. 29(4) (2000), 744–752.

[45] Zou, L., Zhang, W., and Ruan, S., *Modeling the transmission dynamics and control of hepatitis B virus in China*, J. Theor. Biol. 262(2) (2010), 330–338.